

Filteredogenesis of PBH dark matter and baryons

Debasish Borah^{1,2,*} and Indrajit Saha^{1,†}

¹*Department of Physics, Indian Institute of Technology Guwahati, Assam 781039, India*

²*Pittsburgh Particle Physics, Astrophysics,
and Cosmology Center, Department of Physics and Astronomy,
University of Pittsburgh, Pittsburgh, PA 15260, USA*

Abstract

We propose a novel cogenesis of baryon and dark matter (DM) in the Universe by utilising a first-order phase transition (FOPT) in the dark sector containing an asymmetric Dirac fermion χ . Due to the mass difference of χ across the bubble walls, it is energetically favourable for χ to get trapped in the false vacuum leading to the formation of Fermi-ball, which can self-collapse to form primordial black hole (PBH) if χ has a sufficiently large Yukawa interaction. While such PBH formed out of false vacuum collapse can give rise to the DM in the Universe, a tiny amount of asymmetric χ leaking into the true vacuum through the bubble walls can transfer the dark asymmetry into the visible sector via decay. The same mass difference of χ across the two minima which decides the amount of trapping or filtering of χ , also allows χ decay into visible sector in the true minima while keeping it stable in the false vacuum. Our filteredogenesis scenario can be probed via FOPT generated stochastic gravitational waves (GW) at near future detectors in addition to the well-known detection aspects of asteroid mass PBH constituting DM in the Universe.

*Electronic address: dborah@iitg.ac.in

†Electronic address: s.indrajit@iitg.ac.in

I. INTRODUCTION

Observations from cosmology and astrophysics not only indicate the presence of dark matter (DM) in our Universe but also the asymmetric nature of visible matter, known as the baryon asymmetry of Universe (BAU) [1, 2]. The fact that the standard model (SM) of particle physics neither has a DM candidate nor can generate the observed BAU has led to several beyond standard model (BSM) proposals in the literature. Among them, the weakly interacting massive particle (WIMP) [3–5] paradigm for DM and baryogenesis [6, 7] as well as leptogenesis [8] for BAU have been the most popular ones. The strikingly similar abundances of DM (Ω_{DM}) and baryon (Ω_{B}) that is, $\Omega_{\text{DM}} \approx 5 \Omega_{\text{B}}$ in the present Universe has also led to efforts in finding a common origin orogenesis of baryon and DM. Some widely studied cogenesis mechanisms include, but not limited to, asymmetric dark matter [9–16], baryogenesis from DM annihilation [17–30], Affleck-Dine [31] cogenesis [32–37]. Recently, there have also been attempts to generate DM and BAU together via a first-order phase transition (FOPT) by utilising the mass-gain mechanism [38–40] or forbidden decay of DM [41].

While typical baryogenesis or leptogenesis scenarios involve very high scale physics making direct experimental probe difficult, null results at direct detection experiments [42] have pushed WIMP DM scenario to a tight corner. This has led to exploration of DM scenarios beyond the WIMP framework. One such promising alternative is primordial black hole (PBH), recent reviews of which can be found in [43, 44]. PBH with mass in the range $\sim 10^{17} - 10^{22}$ g can be sufficiently stable and free from astrophysical constraints to be a good DM candidate. While PBHs can have their own astrophysical or cosmological signatures, their formation mechanism of also have its own detection aspects. Among well-motivated production mechanisms like PBH from inflationary perturbations [45–50], first-order phase transition [51–64], the collapse of topological defects [65, 66] etc., we consider the FOPT as a source while also connecting it to the origin of BAU in the Universe. This leads to a cogenesis mechanism indirectly testable via FOPT generated stochastic gravitational waves (GW). In particular, we consider the collapsing Fermi-ball scenario [56, 57, 62, 63, 67–71] for PBH formation which also lead to the origin of BAU. A FOPT occurs due to a scalar field which gives a new contribution to a dark fermion mass. The same dark fermion χ with an initial asymmetry gets trapped in the false vacuum due to the mass gap, leading

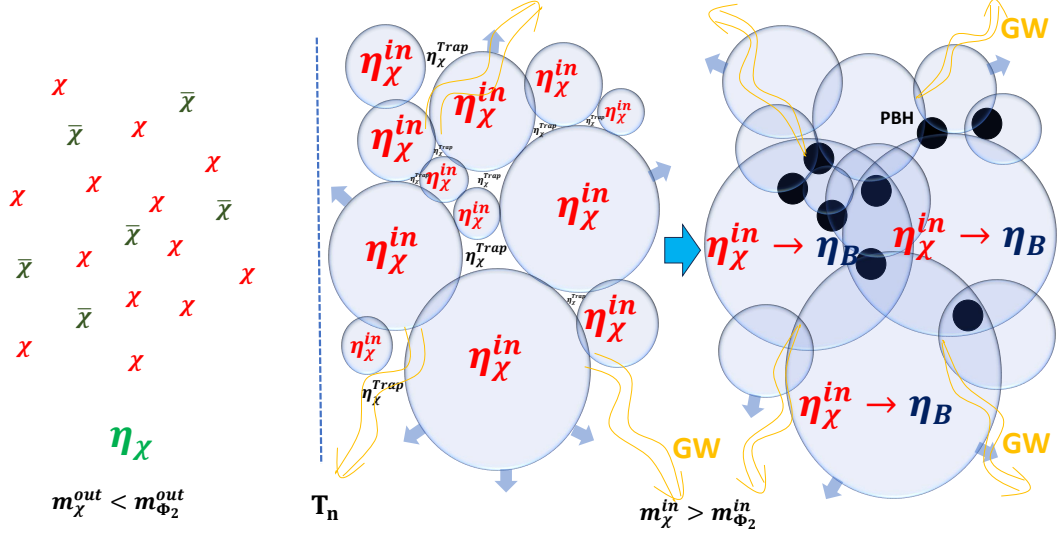


FIG. 1: A schematic diagram of the proposedogenesis scenario.

to the formation of Fermi-balls. These Fermi-balls can further collapse to black holes if there exists an attractive Yukawa force among dark fermions. Since dark fermion maintains equilibrium with the bath prior to the FOPT, its momenta follow an equilibrium distribution allowing some of them to leak into the true vacuum. The enhanced mass of dark fermion in the true vacuum allows its decay into the standard model particles thereby transferring the dark asymmetry into the observed baryon asymmetry. The conceptual visualisation of the idea is summarised in the schematic shown in Fig. 1. Depending upon the scale of the FOPT compared to the sphaleron decoupling temperature, BAU can be generated by direct transfer of dark asymmetry into baryons or via the leptogenesis route. By considering the initial dark asymmetry to be a free parameter, we find a small allowed parameter space consistent with the cogenesis of PBH dark matter and BAU. Coincidentally, this allowed region with nucleation temperature around a few tens to a few hundred GeV remains within the sensitivity of LISA.

This paper is organised as follows. In section II, we discuss the particle physics framework leading to the first-order phase transition. In section III, we discuss the details of filtering or the number of dark fermions leaking into the true vacuum. In section IV we discuss the main results related to cogenesis of PBH dark matter and baryon asymmetry of the Universe. In section V, we outline some UV completions for generating dark fermion asymmetry and finally conclude in section VI.

II. THE FRAMEWORK

We consider a minimal framework consisting of a Dirac singlet fermion χ , two singlet real scalars $\Phi_{1,2}$, three copies of right handed neutrino (RHN) ν_R as the new BSM degrees of freedom. An Z_2 symmetry under which χ, Φ_2 are odd while all other fields are even ensures the stability of the lightest among them. The low energy effective Yukawa Lagrangian relevant for our study is

$$-\mathcal{L} \supset (y_1 \bar{\chi} \Phi_1 \chi + y_2 \bar{\chi} \Phi_2 \nu_R + \text{h.c.}) + m_\chi \bar{\chi} \chi. \quad (1)$$

For simplicity, we consider the light neutrinos to be of Dirac type which acquire mass from a neutrinophilic scalar doublet ζ_1 . Additional symmetries may ensure the pure Dirac nature of light neutrinos while also forbidding neutrino Yukawa coupling with the SM Higgs doublet H . Here we focus on the low energy phenomenology without going into the details of such UV completions [72, 73].

While the singlet scalar Φ_1 drives a first-order phase transition acquiring a non-zero vacuum expectation value (VEV), the other scalars assist in generating the required effective potential while keeping all dimensionless couplings within perturbative limits. We, however, keep the coupling of the SM-like Higgs doublet H with Φ_1 negligible such that the required electroweak symmetry breaking can be achieved independently of this singlet-driven FOPT. With these assumptions, the relevant part of the tree level scalar potential is given by

$$V_{\text{tree}} \supset \lambda_1 \left(\Phi_1^2 - \frac{v_D^2}{2} \right)^2 + \frac{\mu_{\Phi_2}^2}{2} \Phi_2^2 + \frac{\lambda_2}{4} \Phi_2^4 + \frac{\lambda_{\Phi_1 \Phi_2}}{2} \Phi_1^2 \Phi_2^2 + \lambda_{\phi \zeta} \Phi_1^2 |\zeta_1|^2. \quad (2)$$

The other possible terms allowed by the symmetries are ignored for simplicity. The dark fermion receives a new contribution to its mass in the true vacuum $\langle \Phi_1 \rangle = v_D$. This splits the zero-temperature mass of χ inside and outside the bubbles of true vacuum as

$$m_\chi^{\text{in}} = m_\chi + y_1 \frac{v_D}{\sqrt{2}}, \quad m_\chi^{\text{out}} = m_\chi. \quad (3)$$

The one-loop correction to the tree-level potential is calculated by considering the couplings of all particles to the singlet scalar $\Phi_1 = \phi/\sqrt{2}$. This correction, known as the Coleman-Weinberg (CW) potential [74], can be expressed as

$$V_{\text{CW}}(\phi) = \frac{1}{64\pi^2} \sum_{i=\Phi_2, \chi, \zeta} n_i m_i^4(\phi) \left\{ \log \left(\frac{m_i^2(\phi)}{v_D^2} \right) - C_i \right\} \quad (4)$$

where, $n_{\Phi_2} = 1$, $n_\zeta = 4$, $n_\chi = 4$ are the respective degrees of freedom and $C_{\Phi_2, \chi, \zeta} = \frac{3}{2}$. The field dependent masses are

$$m_{\Phi_2}^2(\phi) = \mu_{\Phi_2}^2 + \frac{\lambda_{\Phi_1 \Phi_2} \phi^2}{2}, \quad m_\zeta^2(\phi) = \frac{\lambda_{\phi \zeta} \phi^2}{2}, \quad m_\chi^2(\phi) = (m_\chi + y_1 \phi / \sqrt{2})^2.$$

Now, the thermal contributions to the effective potential [75, 76] can be written as

$$V_T(\phi, T) = \sum_{i=\Phi_2, \zeta} \frac{n_i T^4}{2\pi^2} J_B \left(\frac{m_i^2(\phi)}{T^2} \right) - \frac{n_\chi T^4}{2\pi^2} J_F \left(\frac{m_\chi^2(\phi)}{T^2} \right) \quad (5)$$

where,

$$J_F(x) = \int_0^\infty dy y^2 \log[1 + e^{-\sqrt{y^2+x^2}}], \quad J_B(x) = \int_0^\infty dy y^2 \log[1 - e^{-\sqrt{y^2+x^2}}].$$

In addition, the Daisy corrections [77–79] need to be included in the thermal contribution to enhance the perturbative expansion following the Arnold-Espinosa method [79]. These Daisy contributions can be expressed as

$$V_{\text{daisy}}(\phi, T) = -\frac{T}{2\pi^2} \sum_{i=\Phi_2, \zeta} n_i [m_i^3(\phi, T) - m_i^3(\phi)] \quad (6)$$

where, $m_i^2(\phi, T) = m_i^2(\phi) + \Pi_i(T)$ and the relevant thermal masses are

$$m_{\Phi_2}^2(\phi, T) = m_{\Phi_2}^2(\phi) + \left(\frac{\lambda_2}{4} + \frac{\lambda_{\Phi_1 \Phi_2}}{12} \right) T^2, \quad m_\zeta^2(\phi, T) = m_\zeta^2(\phi) + \left(\frac{\lambda_3}{2} + \frac{\lambda_{\phi \zeta}}{12} \right) T^2.$$

The complete effective finite-temperature potential is

$$V_{\text{eff}}(\phi, T) = V_{\text{tree}}(\phi) + V_{\text{CW}}(\phi) + V_T(\phi, T) + V_{\text{daisy}}(\phi, T). \quad (7)$$

At high temperatures, the Universe stays in the false vacuum $\langle \Phi_1 \rangle = 0$. At the critical temperature T_c another degenerate minimum appears at $\langle \Phi_1 \rangle \neq 0$ with a barrier between them. Subsequently, at a lower temperature known as the nucleation temperature T_n , the Universe tunnels through the barrier to go from the false vacuum to the true vacuum $\langle \Phi_1 \rangle \neq 0$. The tunneling rate per unit volume defined in terms of O(3) symmetric bounce action $S_3(T)$ is $\Gamma(T) \sim T^4 e^{-S_3(T)/T}$ [80]. The nucleation temperature T_n is determined by comparing the tunneling rate with the Hubble expansion rate as

$$\Gamma(T_n) = \mathcal{H}^4(T_n) = \mathcal{H}_*^4. \quad (8)$$

The volume fraction of false vacuum of the Universe is defined by $p(T) = e^{-\mathcal{I}(T)}$ [81, 82], where

$$\mathcal{I}(T) = \frac{4\pi}{3} \int_T^{T_c} \frac{dT'}{T'^4} \frac{\Gamma(T')}{\mathcal{H}(T')} \left(\int_T^{T'} \frac{d\tilde{T}}{\mathcal{H}(\tilde{T})} \right)^3. \quad (9)$$

The percolation temperature T_p is then calculated by using $\mathcal{I}(T_p) = 0.34$ [81] indicating that at least 34% of the comoving volume is occupied by the true vacuum.

The inverse of the FOPT duration is given by $\beta/\mathcal{H} = T \frac{d}{dT} (\frac{S_3}{T})$ while $\alpha_* = \frac{\epsilon}{\rho_{\text{rad}}}$ is amount of latent heat released at nucleation temperature where, $\epsilon = (\Delta V_{\text{eff}} - \frac{T}{4} \frac{\partial \Delta V_{\text{eff}}}{\partial T})_{T=T_n}$, $\Delta V_{\text{eff}} = V_{\text{eff}}(\phi_{\text{false}}, T) - V_{\text{eff}}(\phi_{\text{true}}, T)$ and $\rho_{\text{rad}} = g_* \pi^2 T^4/30$ [83]. The bubble wall velocity v_w , in general, is related to the Jouguet velocity $v_J = \frac{1/\sqrt{3} + \sqrt{\alpha_*^2 + 2\alpha_*/3}}{1 + \alpha_*}$. For the type of FOPT considered here, we can assume $v_w \approx v_J$ [84–86]. The calculation for the bounce action $S_3(T)$ is performed numerically by fitting the effective potential to a generic potential [87], the details of which is described in [39].

We assume the dark fermion to have an initial asymmetry with subsequent annihilation of the symmetric part due to $\chi - \Phi_1$ interactions. In order to trap most of the dark fermions in the false vacuum, we impose the condition $T_n \ll m_\chi^{\text{in}} - m_\chi^{\text{out}}$, such that χ moving to the true vacuum is kinematically disfavored. However, as the momenta of χ follows a distribution, some of them can penetrate to the true vacuum. The same mass gain of χ in true vacuum also allows its decay into ν_R transferring the asymmetry. Since there is no lepton number violation at low scale preserving the pure Dirac nature of light neutrinos, the asymmetry in ν_R is shared with SM leptons due to sizeable Yukawa coupling with then neutrinophilic Higgs doublet. We discuss the trapping of χ in false vacuum andogenesis in the next two sections.

III. FILTERING OF DARK FERMIONS

During a first-order phase transition (FOPT), bubbles of the true vacuum nucleate and expand. Within the bubbles, the symmetry is broken, whereas it remains unbroken outside. Consequently, this results in the mass of the particle χ taking different values inside and outside the bubbles, denoted as m_χ^{in} and m_χ^{out} , respectively. As the bubble expands, χ particles penetrate the bubble wall depending on their energy. Due to the restriction $T_n \ll m_\chi^{\text{in}} - m_\chi^{\text{out}}$, only the high momentum modes of χ can penetrate the walls resulting its filtering.

The idea of bubble filtering has been used in the context of dark matter and baryogenesis in several earlier works [62, 88–94].

Let \tilde{v} denote the velocity of χ particles relative to the bubble wall along z direction, while v_w represents the velocity of the bubble wall in the plasma rest frame. The number of particles per unit area going inside the bubble in time Δt along the z direction can be written in the bubble wall frame following energy conservation as [62, 89]

$$\frac{\Delta N_{\text{in}}}{\Delta A} = n_\chi \int \frac{d^3 p}{(2\pi)^3} \int_{r_o}^{r_o - \frac{p_z \Delta t}{|p|}} dr \mathcal{I}(p) \Theta(-p_z) f(p, x) \quad (10)$$

where ΔA is the area and the energy conservation is ensured by $\mathcal{I}(p) = \Theta(-p_z - m_d)$, $m_d = m_\chi^{\text{in}} - m_\chi^{\text{out}}$, n_χ denotes the degrees of freedom of the particle. Near the bubble wall, χ particles will follow equilibrium distribution locally and hence $f(p, x) \simeq f_{\text{eq}}(p, \tilde{v}, T)$. So, the distribution function outside the bubble is

$$\begin{aligned} f(p, x) &= \frac{1}{e^{\tilde{\gamma}(E - \tilde{v}p_z)/T} + 1} \\ &= \frac{1}{e^{\tilde{\gamma}(\sqrt{p^2 + (m_\chi^{\text{out}})^2} - \tilde{v}p \cos \theta)/T} + 1} \end{aligned} \quad (11)$$

with $\tilde{\gamma}$ being the Lorentz factor. After performing the integration over r , the flux of particles entering the bubble $J_w = \Delta N_{\text{in}}/(\Delta A \Delta t)$ is given by

$$\begin{aligned} J_w &= \frac{n_\chi}{(2\pi)^3} \int d^3 p \Theta(-p_z - m_d) \Theta(-p_z) f(p, x) \left(-\frac{p_z}{|p|} \right) \\ &= \frac{n_\chi}{(2\pi)^3} \int_0^\pi p d\theta \int_0^{2\pi} p \sin \theta d\phi \int_0^\infty dp (-\cos \theta) \Theta(-p \cos \theta - m_d) \Theta(-\cos \theta) f(p) \\ &= \frac{n_\chi}{(2\pi)^2} \int_0^{-1} d(\cos \theta) \cos \theta \int_{-\frac{m_d}{\cos \theta}}^\infty dp \frac{p^2}{e^{\tilde{\gamma}(\sqrt{p^2 + (m_\chi^{\text{out}})^2} - \tilde{v}p \cos \theta)/T} + 1} \\ &= \frac{n_\chi}{(2\pi)^2} \int_0^{-1} dx x \int_{-\frac{m_d}{x}}^\infty dp \frac{p^2}{e^{\tilde{\gamma}(\sqrt{p^2 + (m_\chi^{\text{out}})^2} - \tilde{v}px)/T} + 1}. \end{aligned} \quad (12)$$

Now, the number of particles going inside the bubble with respect to the plasma frame is $n_{\text{in}} = J_w/(\gamma_w v_w)$. Hence, the fraction of particles trapped outside the bubble can be written as

$$F(m_\chi^{\text{out}}, m_\chi^{\text{in}}, T, \tilde{v}, v_w) = 1 - \frac{n_{\text{in}}}{n_{\text{eq}}} \quad (13)$$

From Fig. 2 left panel, it is evident that particle trapping is more efficient when the particles move away from the wall, corresponding to a positive \tilde{v} . Conversely, the trapping efficiency decreases for negative \tilde{v} . However, the trapping function increase with wall velocity, as seen

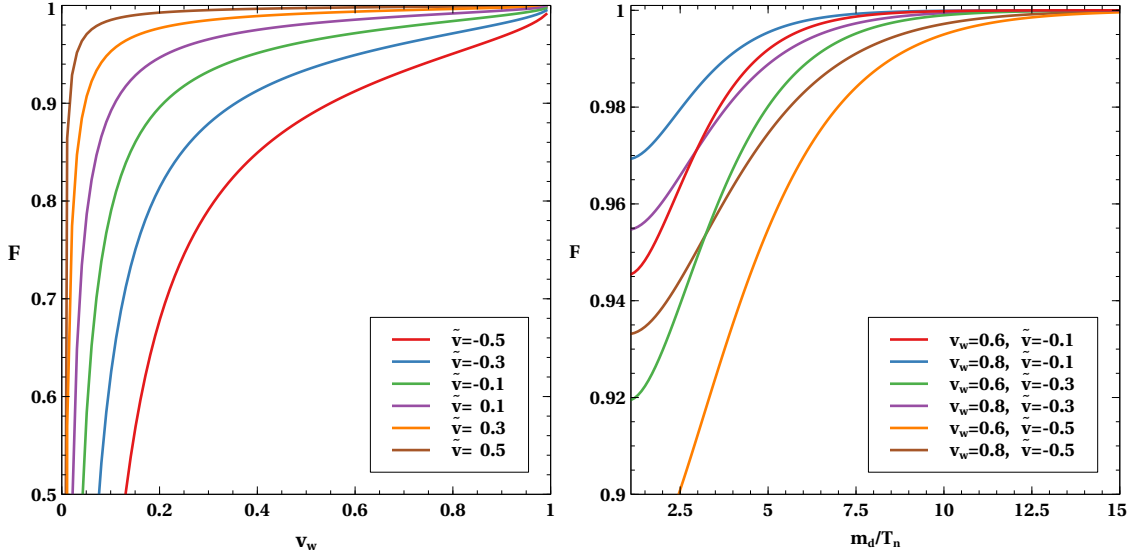


FIG. 2: Left panel: Trapping fraction F versus bubble wall velocity v_w for different values of \tilde{v} , where $m_\chi^{\text{out}} \sim T_n$ and $m_d/T_n \sim 2$. Right panel: Trapping fraction F versus m_d/T_n for different values of \tilde{v} and v_w , where $m_\chi^{\text{out}} \sim T_n$.

from the right panel plot of Fig. 2. The right panel plot also shows the increase of the trapping fraction with the mass gap m_d/T_n as expected. These also agree with the earlier works [62, 89]. For a complete hydrodynamical treatment of bubble and fluid velocities, refer to appendix A.

IV. COGENESIS OF PBH AND BARYON

As the phase transition proceeds via bubble nucleation, the bubbles containing true vacuum grows to cover the entire Universe while the false vacuum regions shrink. Eventually, the false vacuum after shrinking to small disconnected volumes, split further to negligible size at percolation temperature [81]. These squeezed pockets of false vacuum enhance the annihilation of dark fermions [95, 96] leaving only the asymmetric part η_χ . An approximate global charge at low scale ensures the survival of asymmetric dark fermion part in these false vacuum pockets leading to the degeneracy pressure. If the Fermi degeneracy pressure balances the vacuum pressure, it leads to the formation of Fermi-balls at T_* defined by $p(T_*) = 0.29$ [56, 97–99].

The energy of a Fermi-ball can be written as

$$E_{\text{FB}} = \frac{3\pi}{4} \left(\frac{3}{2\pi} \right)^{2/3} \frac{Q_{\text{FB}}^{4/3}}{R} + \frac{4\pi}{3} U_0(T_*) R_{\text{FB}}^3, \quad (14)$$

where, $Q_{\text{FB}} = F_{\chi}^{\text{trap}} \frac{n_{\chi} - n_{\bar{\chi}}}{n_{\text{FB}}^*}$ with n_{χ} denoting number density of χ , $F_{\chi}^{\text{trap}} \approx 1$ for maximum trapping of χ inside false vacuum and U_0 is vacuum energy. Now, minimizing the Fermi-ball energy, we can get the mass and radius as

$$M_{\text{FB}} = Q_{\text{FB}} (12\pi^2 U_0(T_*))^{1/4}, \quad R_{\text{FB}}^3 = \frac{3}{16\pi} \frac{M_{\text{FB}}}{U_0(T_*)}. \quad (15)$$

Within the Fermi-balls, the χ 's interact through attractive Yukawa interaction $g_{\chi} \phi \bar{\chi} \chi$ and the interaction range is $L_{\phi}(T) = \left(\frac{d^2 V_{\text{eff}}}{d\phi^2} \Big|_{\phi=0} \right)^{-1/2}$ [67]. The Yukawa potential energy contribution to the Fermi-ball energy can be expressed as

$$E_Y \simeq -\frac{3g_{\chi}^2 Q_{\text{FB}}^2}{8\pi R_{\text{FB}}} \left(\frac{L_{\phi}}{R_{\text{FB}}} \right)^2. \quad (16)$$

At a later stage, when the Yukawa potential energy becomes larger than the Fermi-ball energy, the Fermi-ball becomes unstable and collapses to form PBH [56]. We consider that the Fermi-ball formation temperature is close to the nucleation temperature, $T_* \sim T_n^1$. The initial PBH mass during formation can be estimated in terms of FOPT parameters as [56]

$$M_{\text{PBH}} \sim 1.4 \times 10^{21} v_w^3 \left(\frac{\eta_{\chi}^{\text{trap}}}{10^{-3}} \right) \left(\frac{100}{g_*} \right)^{1/4} \left(\frac{100 \text{ GeV}}{T_n} \right)^2 \left(\frac{100}{\beta/\mathcal{H}_*} \right)^3 \alpha_*^{1/4} \text{ g} \quad (17)$$

where $\eta_{\chi}^{\text{trap}} = F\eta_{\chi}$ denotes the asymmetric part trapped inside the false vacuum pockets. Primordial black holes, if sufficiently heavy, can contribute to dark matter and its contribution is parametrised as [56]

$$f_{\text{PBH}} = 1.3 * 10^{-3} v_w^{-3} \left(\frac{g_*}{100} \right)^{1/2} \left(\frac{T_n}{100 \text{ GeV}} \right)^3 \left(\frac{\beta/\mathcal{H}_*}{100} \right)^3 \left(\frac{M_{\text{PBH}}}{10^{15} \text{ g}} \right). \quad (18)$$

For PBHs constituting entire DM in the Universe, we have $f_{\text{PBH}} = 1$. PBHs can fully constitute dark matter within the mass range of $9.15 \times 10^{16} \text{ g}$ and $6.70 \times 10^{21} \text{ g}$. The lower bound on mass comes from the evaporation constraint from the cosmic microwave background (CMB) observations [100, 101] while the upper bound on mass comes from the micro-lensing constraint [102].

¹ We also find that the trapping function F remains almost same at T_n and T_* justifying these temperatures to be used interchangeably.

In a co-genesis scenario, the initial dark sector asymmetry helps in the formation of PBH dark matter, while a portion of it filtered through the bubble walls is transferred to baryons or visible sector generating the observed baryon asymmetry of the Universe. As the bubble expands in the Universe, a fraction of the dark asymmetry remains outside the bubble, while the rest passes through the wall and subsequently decays into the visible sector. If the initial asymmetry is partitioned into two components, one contributing to the formation of PBHs, while the other fully converting into the baryon asymmetry, we can write $\eta_\chi = \eta_\chi^{\text{trap}} + \eta_\chi^{\text{in}}$ or $F + \frac{\eta_\chi^{\text{in}}}{\eta_\chi} = 1$.

In Fig. 3, we present the parameter space in $T_n - \eta_\chi$ plane which satisfies the requirements of successful cogogenesis of PBH dark matter and baryon asymmetry. We fix $\beta/\mathcal{H}_* = 40$, $\alpha_* = 0.19$, $v_w = 0.84$ for the left panel and $\beta/\mathcal{H}_* = 80$, $\alpha_* = 0.16$, $v_w = 0.82$ for the right panel of Fig. 3. The solid green line denotes the region where PBHs can account for entire DM. This can be found by using Eq. (17) in Eq. (18) to obtain

$$f_{\text{PBH}} = 5.75 \times 10^2 \alpha_*^{1/4} g_*^{1/4} \left(\frac{F \eta_\chi}{10^{-3}} \right) \left(\frac{T_n}{100} \right) \quad (19)$$

and then setting $f_{\text{PBH}} = 1$. We also calculate the trapping function $F \equiv F(m_\chi^{\text{out}}, m_\chi^{\text{in}}, T_n, \tilde{v}, v_w)$ numerically using Eq. (13), where m_d/T_n is varied from 1 to 50 for each of these points in order to get one-to-one relation between η_χ and T_n in deflagration regime. The black dashed contours are plotted by fixing dark fermion asymmetry leaked to the true vacuum via bubble filtering η_χ^{in} . This allows using $F \eta_\chi = \eta_\chi - \eta_\chi^{\text{in}}$ in Eq. (19) leading to a relation between η_χ and T_n . This is clear from the asymptotic behavior of the black dashed contours as $\eta_\chi \rightarrow \eta_\chi^{\text{in}}$. Only where black dashed contours meet the green solid line, however, the trapping function F corresponds to the exact value calculated in terms of the relevant model parameters $F(m_\chi^{\text{out}}, m_\chi^{\text{in}}, T_n, \tilde{v}, v_w)$. Since the leftmost dashed contour corresponds to $\eta_\chi^{\text{in}} = \eta_B$, the observed baryon asymmetry, the gray meshed region towards the left of the point where it touches the green solid line is disfavored from cogogenesis point of view. For this analysis, we find the local fluid velocity as a function of v_w , considering the deflagration regime as discussed in appendix A and Fig. 9 therein. In Fig. 4, we show the parameter space in $T_n - \eta_\chi$ plane for the same set of parameters as in Fig. 3, considering the detonation regime discussed in appendix A. The detonation regime results in a high local fluid velocity relative to the wall, leading to a wider range of the trapping function F ranging from 0.85 to 1. Consequently, the green region, where PBHs constitute the entire

DM, becomes broader compared to the deflagration regime of Fig. 3.

The orange meshed region in Fig. 3, 4 correspond to the disallowed PBH mass window on lighter side which affects big bang nucleosynthesis (BBN) and the extragalactic photon background [100, 101]. Additionally, the light-green meshed region corresponding to heavier PBH mass is disfavored by HSC-M31 microlensing constraints [102]. The region above the horizontal red-dashed line is disfavored from unitarity upper limit on dark fermion annihilation rate. As the symmetric part of χ is assumed to have annihilated away, it puts an upper bound on $m_\chi \lesssim \mathcal{O}(100)$ TeV, referred to as the unitarity bound [103]. All these constraints finally allow only the white colored regions in Fig. 3, 4 with the cogeneration favored points lying on the green colored band. Different colored points on this band refer to the benchmark points given in table I and table II. The two blue dashed contours represent the LISA sensitivity for PBH mass fixed at the minimum and maximum of the allowed range for it to be DM. The dotted horizontal contour corresponds to the sphaleron decoupling epoch. For points lying below this contour, we require dark fermion asymmetry after bubble filtering to transfer directly into baryons as leptogenesis route gets ineffective due to sphaleron decoupling. Interestingly, all these benchmark points remain within the sensitivities of future GW detector LISA [104]. The stochastic GW spectrum from a FOPT is estimated by considering all the relevant contributions from bubble collisions [105–109], the sound wave [110–113] and the turbulence [84, 114–118] of the plasma medium.

Fig. 5 shows a zoomed-in portion of the allowed region in left panels of Fig. 3 and Fig. 4 indicating the variation of the trapping function F in terms of color code. The left and right panels of Fig. 5 correspond to deflagration and detonation regimes respectively. Clearly, F varies over a wider range in the detonation regime. In the deflagration scenario, the benchmark points BP2 and BP3 satisfy both baryon asymmetry and PBH dark matter scenario. However, in detonation regime, achieving baryon asymmetry is overproduced requiring additional washout in the true vacuum. Fig. 6 shows the GW spectra for the chosen benchmark points given in table I and II. Clearly, all the benchmark points remain within the sensitivities of future experiments like LISA [104], BBO [119] and μ ARES [120].

If the phase transition and bubble filtering of χ occurs before sphaleron decoupling, χ can transfer the asymmetry into neutrinos which can then get converted into baryon asymmetry via electroweak sphalerons. While χ is stable in the false vacuum, it can decay into $\Phi_2\nu_R$ due to the sudden change in mass after the phase transition. In Fig. 7, we can see that χ

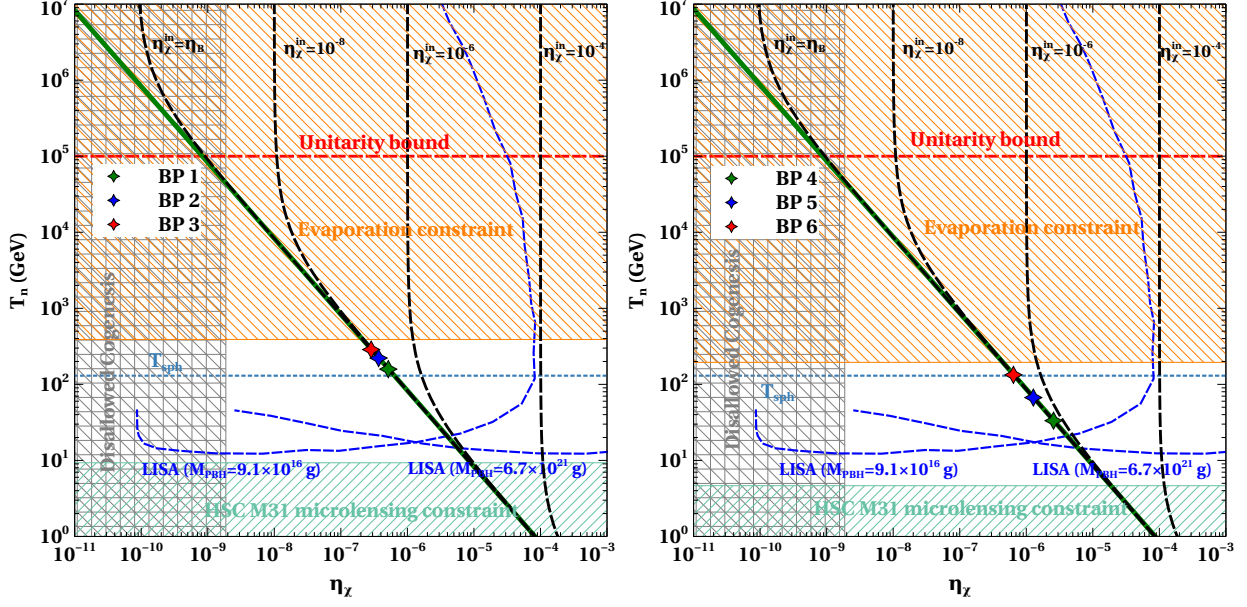


FIG. 3: The parameter space in the η_χ - T_n plane where the solid green line represents condition where PBHs fully constitute dark matter ($f_{\text{PBH}} = 1$) consistent with appropriate bubble filtering. The black dashed lines correspond to the parameter space with fixed dark asymmetry filtered to the true vacuum. For left panel, $\beta/\mathcal{H}_* = 40$, $m_\chi^{\text{out}} \sim T_n$, $\alpha_* = 0.19$ and $v_w = 0.84$ considering deflagration regime. Same for right panel with $\beta/\mathcal{H}_* = 80$, $m_\chi^{\text{out}} \sim T_n$, $\alpha_* = 0.16$ and $v_w = 0.82$.

	v_D (GeV)	μ_{Φ_2} (GeV)	m_{Φ_2} (GeV)	m_χ (GeV)	m_χ^{in} (GeV)	m_{ζ_1} (GeV)	T_c (GeV)	T_n (GeV)	β/\mathcal{H}_*	α_*	M_{PBH} (g)
BP1	1000	300	734.8	150	1139.9	1036.2	267.9	158.5	40	0.19	1.9×10^{18}
BP2	1400	400	1020.7	150	1535.9	1457.2	374.0	221.6	40	0.19	7.0×10^{17}
BP3	1800	500	1306.9	300	2081.9	1852.6	483.9	286.7	40	0.19	3.2×10^{17}

TABLE I: Benchmark points for first-order phase transition.

is stable in a false vacuum, while in a true vacuum, χ can decay such that it transfers the remnant asymmetry to ν_R . Since sphalerons act only on lepton doublets, the asymmetry in ν_R needs to be equilibrated with lepton doublets of the SM. This can happen provided the Dirac Yukawa coupling of neutrinos y_D is sizeable. Demanding this Yukawa interaction to be in equilibrium prior to the sphaleron decoupling epoch leads to a lower bound

$$T y_D^2 \gtrsim \sqrt{\frac{\pi^2}{90}} g_* \frac{T^2}{M_{\text{Pl}}} \implies y_D \gtrsim 10^{-8}. \quad (20)$$

The asymmetry generated in ν_R is then transferred to left-handed leptons via sizeable coupling with neutrinophilic Higgs doublet ζ_1 . If this asymmetry is transferred to the left-handed

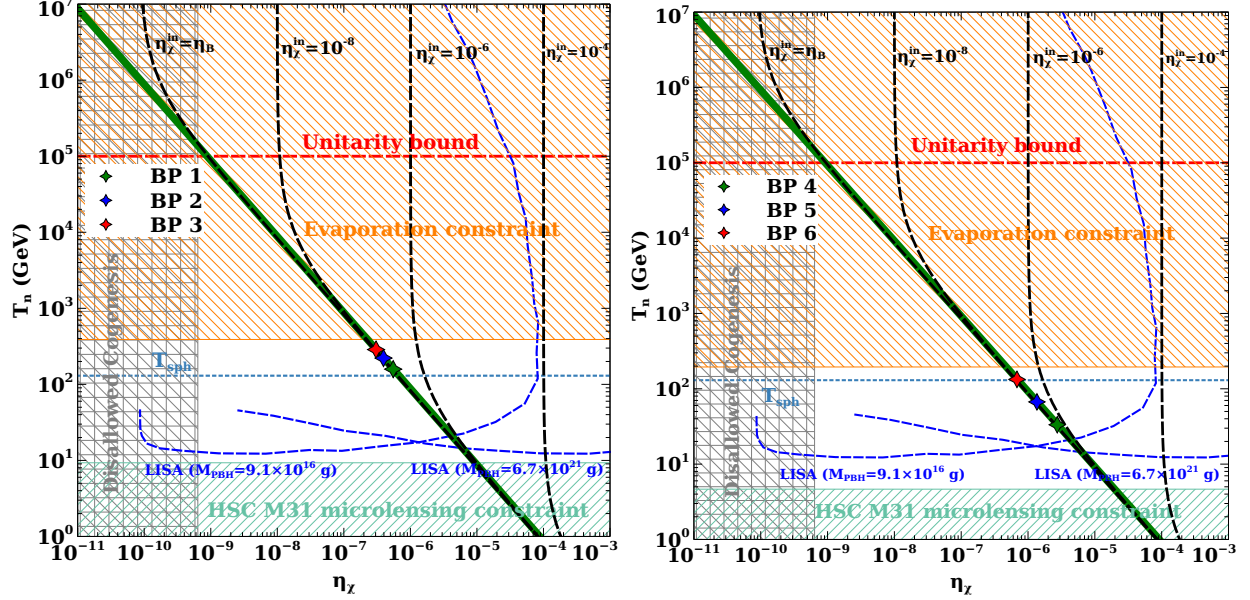


FIG. 4: The parameter space in the η_χ - T_n plane where the solid green line represents condition where PBHs fully constitute dark matter ($f_{\text{PBH}} = 1$) consistent with appropriate bubble filtering. The black dashed lines correspond to the parameter space with fixed dark asymmetry filtered to the true vacuum. For left panel, $\beta/\mathcal{H}_* = 40$, $m_\chi^{\text{out}} \sim T_n$, $\alpha_* = 0.19$ and $v_w = 0.84$ considering detonation regime. Same for right panel with $\beta/\mathcal{H}_* = 80$, $m_\chi^{\text{out}} \sim T_n$, $\alpha_* = 0.16$ and $v_w = 0.82$.

	v_D (GeV)	μ_{Φ_2} (GeV)	m_{Φ_2} (GeV)	m_χ (GeV)	m_χ^{in} (GeV)	m_{ζ_1} (GeV)	T_c (GeV)	T_n (GeV)	β/\mathcal{H}_*	α_*	M_{PBH} (g)
BP4	200	100	167.3	40	237.9	205.5	53.9	33.3	80	0.16	2.4×10^{19}
BP5	400	200	334.6	80	475.9	410.0	108.2	67.0	80	0.16	2.9×10^{18}
BP6	800	300	614.8	100	891.6	832.0	214.9	133.3	80	0.16	3.7×10^{17}

TABLE II: Benchmark points for first-order phase transition.

leptons before sphalerons decouple, a non-zero baryon asymmetry can be generated. Neutrinos acquire small Dirac mass at tree level from the VEV of the neutral component of ζ_1 (denoted by v_2) as

$$M_D = \frac{y_D v_2}{\sqrt{2}} \quad (21)$$

where v_2 can be much smaller than the VEV of the SM-like Higgs doublet H . This can be achieved if the VEV of ζ_1 is protected by an approximate global symmetry and can only be induced after electroweak symmetry breaking due to the VEV of H . Smallness of v_2 compared to $v_1 \equiv \langle H \rangle$ ensures that the Yukawa coupling y_D is sufficiently large to transfer

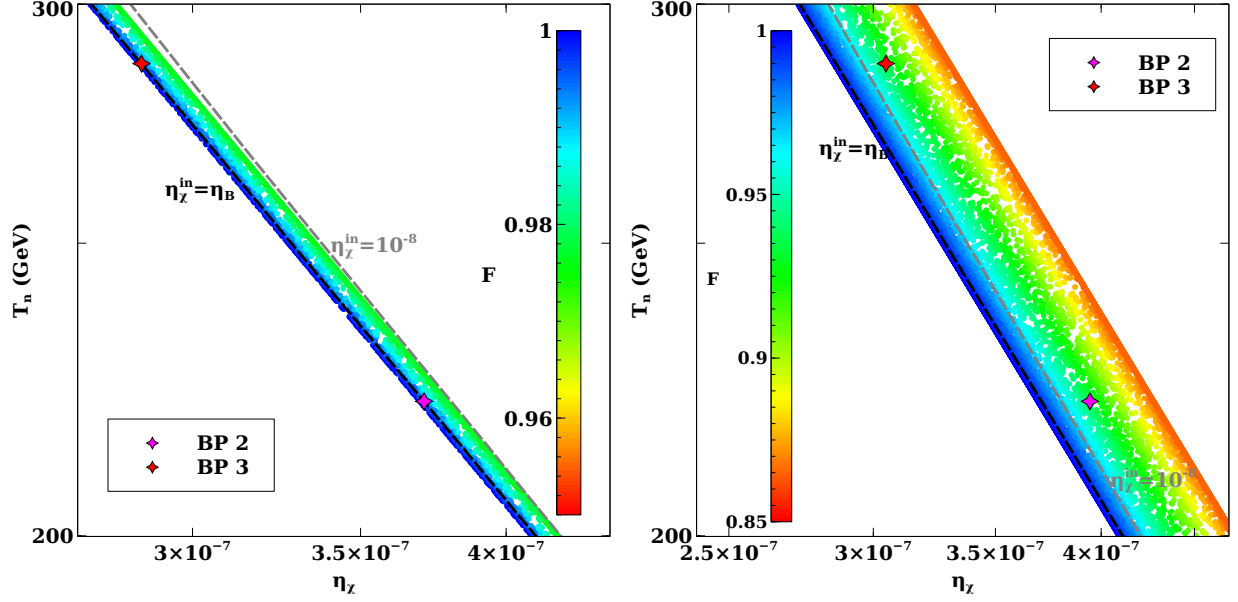


FIG. 5: The parameter space in the η_χ - T_n plane with trapping fraction F in color code where PBHs fully constitute dark matter ($f_{\text{PBH}} = 1$) consistent with appropriate bubble filtering. The black and gray dashed lines correspond to the parameter space with fixed dark asymmetry filtered to the true vacuum. For $\beta/\mathcal{H}_* = 40$, $m_\chi^{\text{out}} \sim T_n$, $\alpha_* = 0.19$ and $v_w = 0.84$, left and right panel correspond to deflagration and detonation regime respectively.

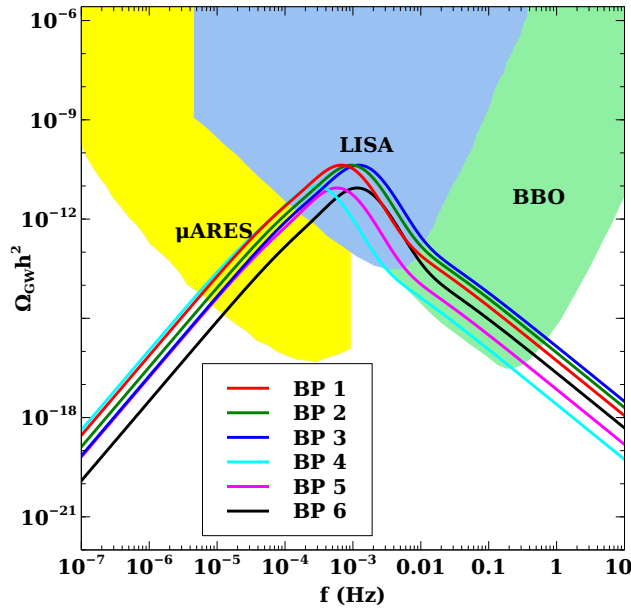


FIG. 6: Gravitational wave spectrum corresponding to benchmark points in Table I and II.

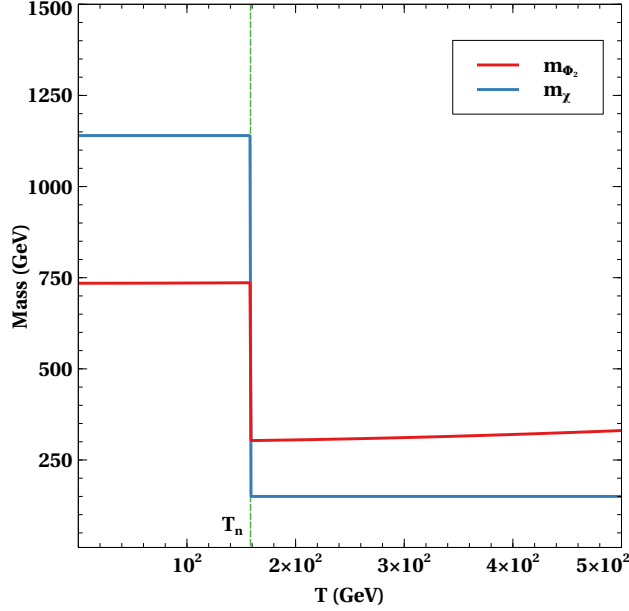


FIG. 7: Thermal mass profiles of dark fermion χ and scalar Φ_2 corresponding to the benchmark point BP1 in Table I.

the asymmetry from ν_R to ν_L . Thus ζ_1 not only assist in Φ_1 -driven FOPT but also make leptogenesis and light neutrino mass viable.

Since dark fermion stores an asymmetry much larger than the observed baryon asymmetry, it is also required to ensure that they do not transfer the asymmetry to leptons via scattering processes like $\chi\Phi_2 \rightarrow l\zeta_1$ mediated by ν_R . Keeping this lepton number conserving $\Delta L = 0$ conversion process out-of-equilibrium at a temperature T leads to

$$T \frac{y_D^2 y_2^2}{4\pi} \lesssim \sqrt{\frac{\pi^2}{90} g_*} \frac{T^2}{M_{\text{Pl}}}, \quad (22)$$

assuming massless initial and final states appropriate for high temperatures. Demanding this process to be out-of-equilibrium at a nucleation temperature as low as electroweak scale puts the most conservative bound $y_D^2 y_2^2 \lesssim 10^{-16}$ which can be satisfied by suitable choice of y_2 while being in agreement with the lower bound on y_D mentioned in Eq. (20). For example, among the relevant benchmark points, BP1, BP2 and BP3 require $y_2 \sim 10^{-6}$, while for BP6 $y_2 \sim 10^{-5}$. Such Yukawa couplings keep the transfer of dark fermion asymmetry to leptons via scattering naturally suppressed.

The singlet scalar Φ_2 produced from χ decay in true vacuum can be made irrelevant cosmologically if allowed to decay into the SM particles via soft Z_2 -breaking terms. In

the unbroken Z_2 limit, it is possible to tune Φ_2 mass and scalar portal couplings in such a way that its abundance remain below DM abundance. In a scenario where $f_{\text{PBH}} < 1$, the remaining fraction of DM can arise from Φ_2 . However, in the present work, we ignore this possibility and assume Φ_2 abundance to be negligible in true vacuum. For low scale phase transition with $T_n < T_{\text{sph}}$, dark fermion asymmetry after bubble filtering needs to be transferred directly to baryons. This requires different model building approach beyond the scope of this present work.

V. POSSIBLE ORIGIN OF DARK ASYMMETRY

In the above discussions, we have considered dark fermion asymmetry as an initial condition. The minimal framework we adopted can not generate this asymmetry. There are various ways of generating dark sector asymmetries as studied in asymmetric dark matter scenarios [9, 10, 13–16, 36, 37, 121–130]. Here, for simplicity, we outline one such UV completion based on the Affleck-Dine (AD) mechanism [31].

Consider an Affleck-Dine field η singlet under the SM gauge symmetry but having a global $U(1)_L$ charge 2. The Dirac fermion χ has global charge 1. The relevant terms involving η, χ can be written as

$$-\mathcal{L} \supset Y_D \bar{\chi}^c \chi \eta^\dagger + \epsilon \mu^2 \eta^2 + \text{h.c.} \quad (23)$$

While ν_R also has lepton number 1, we can prevent direct coupling of η with ν_R via discrete symmetries like $Z_N, N > 2$. Depending upon Z_N charge of ν_R , one can choose the corresponding Z_N charges of Φ_2, ζ_1 as well. We skip these details as they do not affect the generation of χ asymmetry. While the Yukawa interaction in Eq. (23) preserves $U(1)_L$, the $\epsilon \mu^2 \eta^2$ term of the AD field explicitly breaks $U(1)_L$. Due to this explicit lepton number violating term, the cosmological evolution of the AD field leads to a generation of non-zero lepton number, which gets transferred to the dark fermion χ when η decays into them. Assuming the decay of the AD field also to reheat the Universe to a temperature $T_{\text{RH}} \simeq \sqrt{\Gamma_\eta M_{\text{Pl}}}$, the dark fermion asymmetry can be estimated as [36, 131, 132]

$$Y_{\Delta\chi}^{\text{in}} = \frac{(n_\chi - n_{\bar{\chi}})}{s} \simeq \frac{T_{\text{RH}}^3}{\epsilon m_\eta^2 M_{\text{Pl}}} \quad (24)$$

where m_η is the mass of the AD field. The dominant washout process is the one which breaks $U(1)_L$ by 4 units: $\chi\chi \leftrightarrow \bar{\chi}\bar{\chi}$ mediated by η . Keeping this washout out-of-equilibrium leads

to the following condition

$$T_{\text{RH}}^3 \frac{Y_D^4 \epsilon^2 T_{\text{RH}}^2}{4\pi m_\eta^4} \lesssim \sqrt{\frac{\pi^2}{90} g_*} \frac{T_{\text{RH}}^2}{M_{\text{Pl}}}, \quad (25)$$

which can be ensured by suitable choices of couplings and masses.

VI. CONCLUSION

We have proposed a novelogenesis mechanism of producing dark matter and baryon asymmetry in the Universe by utilising a first-order phase transition in the early Universe. The FOPT driven by a singlet scalar also leads to a sharp rise in a dark fermion mass. While the dark fermion remains in equilibrium prior to the FOPT, a large mass gap across the bubble wall $m_d \gg T_n$ prevents most of these dark fermions to get trapped in the false vacuum. An initial dark sector asymmetry prevents the dark fermions from being annihilated away in the squeezed pockets of false vacuum. While such false vacuum pockets lead to the formation of Fermi-balls when Fermi degeneracy pressure balances the vacuum pressure, a strong attractive Yukawa type interaction among dark fermions can induce further collapse to primordial black holes. Since the dark fermion momenta follow equilibrium distribution prior to the FOPT, its high momentum modes are energetic enough to leak into the true vacuum through the bubble walls, leading to filtering of dark fermions. The filtered dark fermion can also decay into the visible sector due to the mass gain in the true vacuum, thereby transferring the filtered dark sector asymmetry to visible sector asymmetry. We constrain the model from the requirement of producing the observed dark matter relic in the form of PBHs and observed baryon asymmetry from filtered dark sector asymmetry in the true vacuum. We find a small allowed region of parameter space with nucleation temperature ranging from a few tens of GeV to a few hundred GeV which is consistent with the cogenesis requirements and experimental bounds on PBH mass. Interestingly, for this allowed region of parameter space, the FOPT generated stochastic gravitational wave remains within reach of future GW experiments like LISA. Additionally, such sub-TeV scale FOPT scenario has several light new degrees of freedom accessible at terrestrial experiments. The PBHs in this asteroid mass range can also have their own observational signatures related superradiance, Hawking evaporation or microlensing [133]. While we have performed our detailed numerical analysis assuming an initial dark sector asymmetry, we also outline one possible UV completion where such an asymmetry can be generated at a

scale above the phase transition scale via the Affleck-Dine mechanism. If the FOPT occurs prior to the sphaleron decoupling epoch, the dark sector asymmetry can be transferred to leptons as we have shown in our minimal framework. This lepton asymmetry can then be converted into baryon asymmetry via electroweak sphalerons. However, if the FOPT occurs below the sphaleron decoupling, dark sector asymmetry needs to be converted directly into baryons requiring different model building approach which we leave for future works.

Acknowledgments

We thank Arnab Dasgupta for useful discussions. The work of D.B. is supported by the Science and Engineering Research Board (SERB), Government of India grants MTR/2022/000575 and CRG/2022/000603. D.B. also acknowledges the support from the Fulbright-Nehru Academic and Professional Excellence Award 2024-25.

Appendix A: Hydrodynamical treatment of velocities

As the first-order phase transition progresses, the expanding bubble releases latent heat into the radiation bath of the Universe, generating velocity and temperature profiles of the fluid across the bubble wall. In this section, we discuss the dynamics of wall velocity. The energy-momentum tensor of the scalar field that drives the phase transition is

$$T_{\alpha\beta}^{\phi} = \partial_{\alpha}\phi\partial_{\beta}\phi - g_{\alpha\beta} \left[\frac{1}{2}\partial_{\mu}\phi\partial^{\mu}\phi - V_{\text{eff}}(\phi) \right]. \quad (\text{A1})$$

On the other hand, the energy-momentum tensor of the plasma is given by

$$T_{\alpha\beta}^{\text{pl}} = \sum_i \int \frac{d^3k}{(2\pi)^3 E_i} k_{\alpha} k_{\beta} f_i(k, x), \quad (\text{A2})$$

where, the i index corresponds to each species in the plasma. Assuming the plasma to be locally in thermal equilibrium, its energy-momentum tensor can be expressed as that of a perfect fluid,

$$T_{\alpha\beta}^{\text{pl}} = w_{\text{pl}} u_{\alpha} u_{\beta} - g_{\alpha\beta} p_{\text{pl}}, \quad (\text{A3})$$

where w_{pl} , p_{pl} and $u_{\alpha} \equiv \gamma(1, \mathbf{v})$ are plasma enthalpy, pressure and four-velocity respectively. With the ϕ background contributing to total pressure, the total fluid energy-momentum

tensor can be written as

$$T_{\alpha\beta}^{\text{fl}} = T_{\alpha\beta}^{\phi} + T_{\alpha\beta}^{\text{pl}} = wu_{\alpha}u_{\beta} - g_{\alpha\beta}p, \quad (\text{A4})$$

where, the enthalpy $w = T \frac{\partial p}{\partial T}$ and the energy density $e = T \frac{\partial p}{\partial T} - p = w - p$. The conservation of energy-momentum leads to $\partial^{\alpha} T_{\alpha\beta}^{\text{fl}} = 0$. For a constant bubble wall velocity, the time-independent components of the energy-momentum conservation equations in bubble wall frame can be expressed as [86, 94]

$$\partial_z T^{zz} = \partial_z T^{z0} = 0 \quad (\text{A5})$$

where z -axis is chosen to be direction of bubble and fluid velocities. From the above equation, we get the matching equations across the bubble wall as follows

$$w_f v_f^2 \gamma_f + p_f = w_t v_t^2 \gamma_t + p_t \quad \text{and} \quad w_f v_f \gamma_f^2 = w_t v_t \gamma_t^2, \quad (\text{A6})$$

here, subscripts t and f represent inside the bubble (true vacuum) and outside the bubble (false vacuum), respectively. In the relativistic gas approximation of plasma, the equation of state outside the bubble can be written as

$$p_f = \frac{1}{3} a_f T_f^4 - \epsilon, \quad e_f = a_f T_f^4 + \epsilon, \quad (\text{A7})$$

where, ϵ is the false vacuum energy and a correspond to degrees of freedom across the wall. While inside the bubble

$$p_t = \frac{1}{3} a_t T_t^4, \quad e_t = a_t T_t^4. \quad (\text{A8})$$

After substituting Eq. (A7) and Eq. (A8) in Eq. (A6), we get

$$v_f v_t = \frac{1 - (1 - \alpha_*)\rho}{3 - 3(1 + \alpha_*)\rho}, \quad \frac{v_f}{v_t} = \frac{3 + (1 - 3\alpha_*)\rho}{1 + 3(1 + \alpha_*)\rho}, \quad (\text{A9})$$

where, $\alpha_* = \epsilon / (a_f T_f^4)$, $\rho = a_f T_f^4 / (a_t T_t^4)$. Then, combining the above two equations, we get

$$v_f = \frac{1}{1 + \alpha_*} \left[\left(\frac{v_t}{2} + \frac{1}{6v_t} \right) \pm \sqrt{\left(\frac{v_t}{2} + \frac{1}{6v_t} \right)^2 + \alpha_*^2 + \frac{2}{3}\alpha_* - \frac{1}{3}} \right]. \quad (\text{A10})$$

There are two branches of solutions corresponding to the \pm signs on the right hand side of Eq. (A10). The positive branch solution belongs to detonation, $v_f > v_t$ and the negative branch solution gives deflagration, $v_f < v_t$. Connecting with the discussion in section III,

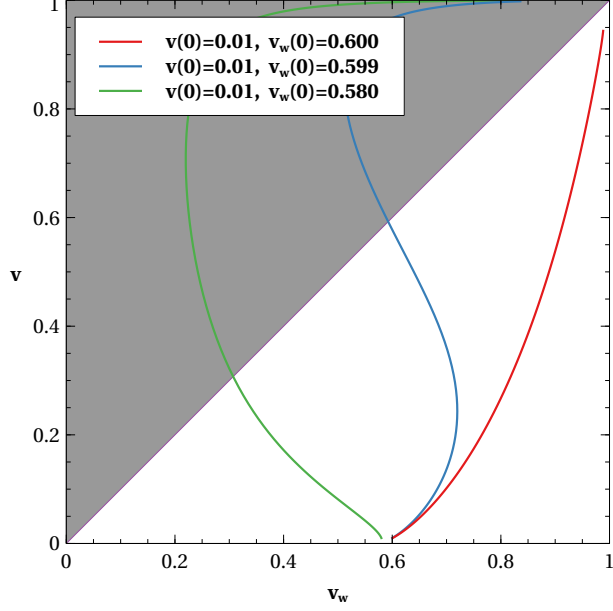


FIG. 8: Generic fluid velocity profile with corresponding wall velocity $v_w = \xi$.

v_f represents the velocity of the fluid in front of the wall i.e. \tilde{v} , while v_t denotes the velocity of the fluid behind the wall, both measured in the wall rest frame. We now calculate the bubble wall velocity and the corresponding velocity of the fluid moving behind the wall from plasma frame of reference. The conservation equation can be written as

$$\partial_\alpha T^{\alpha\beta} = u^\beta \partial_\alpha (u^\alpha w) + u^\alpha w \partial_\alpha u^\beta - \partial^\beta p. \quad (\text{A11})$$

Taking the projection along the flow, leads to

$$\partial(u^\alpha w) - u_\alpha \partial^\alpha p = 0. \quad (\text{A12})$$

Now, taking the projection perpendicular to the flow with $\bar{u}_\alpha \equiv \gamma(v, v/v)$, we get

$$\bar{u}^\alpha u^\beta w \partial_\alpha u_\beta - \bar{u}^\beta \partial_\beta p = 0. \quad (\text{A13})$$

In the absence of a characteristic distance scale, the solution is expected to depend on the self-similar parameter $\xi = r/t$, where r is the distance from the center of the bubble, and t is the time elapsed since nucleation. The gradients can be defined as

$$u_\alpha \partial^\alpha = -\frac{\gamma}{t}(\xi - v)\partial_\xi, \quad \bar{u}_\alpha \partial^\alpha = \frac{\gamma}{t}(1 - \xi v)\partial_\xi. \quad (\text{A14})$$

From Eq. (A12) and Eq. (A13), we get

$$(\xi - v)\frac{\partial_\xi e}{w} = 2\frac{v}{\xi} + \{1 - \gamma^2 v(\xi - v)\}\partial_\xi v, \quad (1 - v\xi)\frac{\partial_\xi p}{w} = \gamma^2(\xi - v)\partial_\xi v. \quad (\text{A15})$$

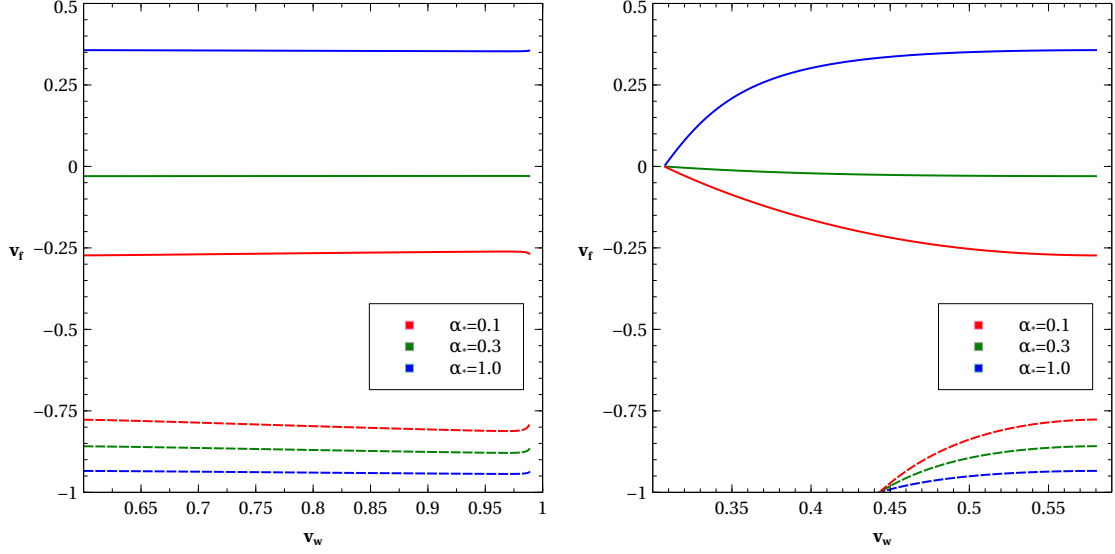


FIG. 9: Left panel: local fluid velocity in front of the wall, v_f versus bubble wall velocity for different values of α_* corresponding to the red colored profile of Fig. 8. Right panel: same as the left panel but corresponding to the green colored profile of Fig. 8. The solid and dashed lines correspond to deflagration and detonation regimes, respectively.

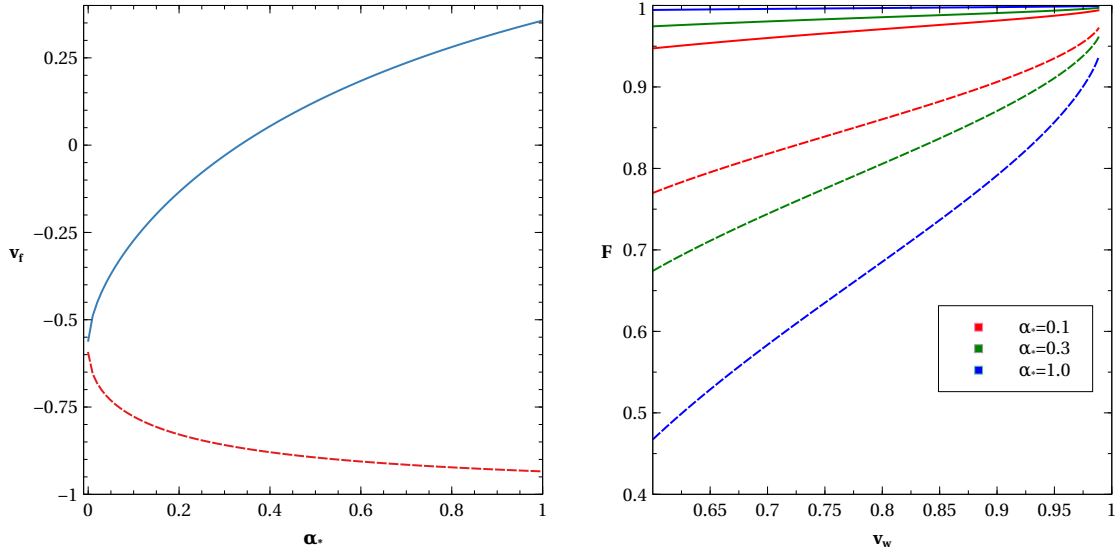


FIG. 10: Left panel: Local fluid velocity in front of wall, v_f versus α_* , Right panel: Fraction of trapped particles F versus bubble wall velocity, v_w corresponding to the left panel of Fig. 9. The solid and dashed lines correspond to deflagration and detonation regimes, respectively.

Using the definition of the sound speed of the plasma $c_s^2 \equiv (dp/dT)/(de/dT)$, the above two equations can be expressed as

$$2\frac{v}{\xi} = \gamma^2(1 - v\xi)\left(\frac{\mu^2}{c_s^2} - 1\right)\partial_\xi v, \quad (\text{A16})$$

where, $\mu = (\xi - v)/(1 - \xi v)$. The above equation can be solved by introducing an auxiliary parameter τ , which helps to write the equation as

$$\frac{dv}{d\tau} = 2vc_s^2(1 - v^2)(1 - \xi v), \quad \frac{d\xi}{d\tau} = \xi((\xi - v)^2 - c_s^2(1 - \xi v)^2), \quad (\text{A17})$$

and the solutions for various initial conditions are illustrated in Fig. 8. Here, we show three types of profiles corresponding to the green, blue and red colored contours respectively. The gray shaded upper triangular region in the does not provide physically consistent solutions.

The fluid velocity behind the wall is v in the plasma frame, whereas it is v_t in the wall's rest frame. We can write $v = (v_t + v_w)/(1 + v_t v_w)$ using Lorentz transformation of velocities. Thus, v_w can be expressed as a function $f(v_f)$ in terms of the local plasma velocity in front of the wall, measured in the wall's rest frame. In Fig. 9, we connect the local fluid velocity with wall velocity, with solid and dashed lines corresponding to deflagration and detonation regimes, respectively. From the left panel of Fig. 9, we can see that v_f is nearly independent of the wall velocity v_w , while it depends on α_* shown in the left panel of Fig. 10. In the right panel of Fig. 10, we show the fraction of particles trapped outside the bubble as a function of wall velocity, where $m_\chi^{\text{out}} \sim T_n$, $m_\chi^{\text{in}} \sim 2T_n$ corresponding to the left panel of Fig. 9. We use these dependence of fluid and bubble velocities while calculating the trapping function F relevant for cogenesis discussed in section IV.

-
- [1] PARTICLE DATA GROUP collaboration, *Review of Particle Physics*, *PTEP* **2020** (2020) 083C01.
 - [2] PLANCK collaboration, *Planck 2018 results. VI. Cosmological parameters*, **1807.06209**.
 - [3] E.W. Kolb and M.S. Turner, *The Early Universe*, vol. 69 (1990).
 - [4] G. Jungman, M. Kamionkowski and K. Griest, *Supersymmetric dark matter*, *Phys. Rept.* **267** (1996) 195 [[hep-ph/9506380](#)].
 - [5] G. Bertone, D. Hooper and J. Silk, *Particle dark matter: Evidence, candidates and constraints*, *Phys. Rept.* **405** (2005) 279 [[hep-ph/0404175](#)].

- [6] S. Weinberg, *Cosmological Production of Baryons*, *Phys. Rev. Lett.* **42** (1979) 850.
- [7] E.W. Kolb and S. Wolfram, *Baryon Number Generation in the Early Universe*, *Nucl. Phys.* **B172** (1980) 224.
- [8] M. Fukugita and T. Yanagida, *Baryogenesis Without Grand Unification*, *Phys. Lett.* **B174** (1986) 45.
- [9] S. Nussinov, *TECHNOCOSMOLOGY: COULD A TECHNIBARYON EXCESS PROVIDE A 'NATURAL' MISSING MASS CANDIDATE?*, *Phys. Lett. B* **165** (1985) 55.
- [10] H. Davoudiasl and R.N. Mohapatra, *On Relating the Genesis of Cosmic Baryons and Dark Matter*, *New J. Phys.* **14** (2012) 095011 [[1203.1247](#)].
- [11] K. Petraki and R.R. Volkas, *Review of asymmetric dark matter*, *Int. J. Mod. Phys. A* **28** (2013) 1330028 [[1305.4939](#)].
- [12] K.M. Zurek, *Asymmetric Dark Matter: Theories, Signatures, and Constraints*, *Phys. Rept.* **537** (2014) 91 [[1308.0338](#)].
- [13] A. Dutta Banik, R. Roshan and A. Sil, *Neutrino mass and asymmetric dark matter: study with inert Higgs doublet and high scale validity*, [2011.04371](#).
- [14] B. Barman, D. Borah, S.J. Das and R. Roshan, *Non-thermal origin of asymmetric dark matter from inflaton and primordial black holes*, *JCAP* **03** (2022) 031 [[2111.08034](#)].
- [15] Y. Cui and M. Shamma, *WIMP Cogenesis for Asymmetric Dark Matter and the Baryon Asymmetry*, *JHEP* **12** (2020) 046 [[2002.05170](#)].
- [16] D. Borah, S. Mahapatra, P.K. Paul, N. Sahu and P. Shukla, *Asymmetric self-interacting dark matter with a canonical seesaw model*, *Phys. Rev. D* **110** (2024) 035033 [[2404.14912](#)].
- [17] M. Yoshimura, *Unified Gauge Theories and the Baryon Number of the Universe*, *Phys. Rev. Lett.* **41** (1978) 281.
- [18] S.M. Barr, *Comments on Unitarity and the Possible Origins of the Baryon Asymmetry of the Universe*, *Phys. Rev. D* **19** (1979) 3803.
- [19] I. Baldes, N.F. Bell, K. Petraki and R.R. Volkas, *Particle-antiparticle asymmetries from annihilations*, *Phys. Rev. Lett.* **113** (2014) 181601 [[1407.4566](#)].
- [20] X. Chu, Y. Cui, J. Pradler and M. Shamma, *Dark freeze-out cogenesis*, *JHEP* **03** (2022) 031 [[2112.10784](#)].
- [21] Y. Cui, L. Randall and B. Shuve, *A WIMPy Baryogenesis Miracle*, *JHEP* **04** (2012) 075 [[1112.2704](#)].

- [22] N. Bernal, F.-X. Josse-Michaux and L. Ubaldi, *Phenomenology of WIMP_y baryogenesis models*, *JCAP* **01** (2013) 034 [[1210.0094](#)].
- [23] N. Bernal, S. Colucci, F.-X. Josse-Michaux, J. Racker and L. Ubaldi, *On baryogenesis from dark matter annihilation*, *JCAP* **10** (2013) 035 [[1307.6878](#)].
- [24] J. Kumar and P. Stengel, *WIMP_y Leptogenesis With Absorptive Final State Interactions*, *Phys. Rev. D* **89** (2014) 055016 [[1309.1145](#)].
- [25] J. Racker and N. Rius, *Helicitogenesis: WIMP_y baryogenesis with sterile neutrinos and other realizations*, *JHEP* **11** (2014) 163 [[1406.6105](#)].
- [26] A. Dasgupta, C. Hati, S. Patra and U. Sarkar, *A minimal model of TeV scale WIMP_y leptogenesis*, [1605.01292](#).
- [27] D. Borah, A. Dasgupta and S.K. Kang, *TeV Scale Leptogenesis via Dark Sector Scatterings*, *Eur. Phys. J. C* **80** (2020) 498 [[1806.04689](#)].
- [28] D. Borah, A. Dasgupta and S.K. Kang, *Two-component dark matter with cogeneration of the baryon asymmetry of the Universe*, *Phys. Rev. D* **100** (2019) 103502 [[1903.10516](#)].
- [29] A. Dasgupta, P.S. Bhupal Dev, S.K. Kang and Y. Zhang, *New mechanism for matter-antimatter asymmetry and connection with dark matter*, *Phys. Rev. D* **102** (2020) 055009 [[1911.03013](#)].
- [30] D. Mahanta and D. Borah, *WIMP_y leptogenesis in non-standard cosmologies*, *JCAP* **03** (2023) 049 [[2208.11295](#)].
- [31] I. Affleck and M. Dine, *A New Mechanism for Baryogenesis*, *Nucl. Phys. B* **249** (1985) 361.
- [32] L. Roszkowski and O. Seto, *Axino dark matter from Q-balls in Affleck-Dine baryogenesis and the $\Omega(b) - \Omega(DM)$ coincidence problem*, *Phys. Rev. Lett.* **98** (2007) 161304 [[hep-ph/0608013](#)].
- [33] O. Seto and M. Yamaguchi, *Axino warm dark matter and $\Omega(b) - \Omega(DM)$ coincidence*, *Phys. Rev. D* **75** (2007) 123506 [[0704.0510](#)].
- [34] C. Cheung and K.M. Zurek, *Affleck-Dine Cogeneration*, *Phys. Rev. D* **84** (2011) 035007 [[1105.4612](#)].
- [35] B. von Harling, K. Petraki and R.R. Volkas, *Affleck-Dine dynamics and the dark sector of pangenesis*, *JCAP* **05** (2012) 021 [[1201.2200](#)].
- [36] D. Borah, S. Jyoti Das and N. Okada, *Affleck-Dine cogeneration of baryon and dark matter*, *JHEP* **05** (2023) 004 [[2212.04516](#)].

- [37] D. Borah, S. Jyoti Das and R. Roshan, *Baryon asymmetry from dark matter decay*, *Phys. Rev. D* **108** (2023) 075025 [2305.13367].
- [38] I. Baldes, S. Blasi, A. Mariotti, A. Sevrin and K. Turbang, *Baryogenesis via relativistic bubble expansion*, *Phys. Rev. D* **104** (2021) 115029 [2106.15602].
- [39] D. Borah, A. Dasgupta and I. Saha, *Leptogenesis and dark matter through relativistic bubble walls with observable gravitational waves*, *JHEP* **11** (2022) 136 [2207.14226].
- [40] D. Borah, A. Dasgupta and I. Saha, *LIGO-Virgo constraints on dark matter and leptogenesis triggered by a first order phase transition at high scale*, *Phys. Rev. D* **109** (2024) 095034 [2304.08888].
- [41] D. Borah, A. Dasgupta, M. Knauss and I. Saha, *Baryon asymmetry from dark matter decay in the vicinity of a phase transition*, *Phys. Rev. D* **108** (2023) L091701 [2306.05459].
- [42] LZ collaboration, *First Dark Matter Search Results from the LUX-ZEPLIN (LZ) Experiment*, *Phys. Rev. Lett.* **131** (2023) 041002 [2207.03764].
- [43] B. Carr, K. Kohri, Y. Sendouda and J. Yokoyama, *Constraints on primordial black holes*, *Rept. Prog. Phys.* **84** (2021) 116902 [2002.12778].
- [44] B. Carr and F. Kuhnel, *Primordial black holes as dark matter candidates*, *SciPost Phys. Lect. Notes* **48** (2022) 1 [2110.02821].
- [45] S. Hawking, *Gravitationally collapsed objects of very low mass*, *Mon. Not. Roy. Astron. Soc.* **152** (1971) 75.
- [46] B.J. Carr and S.W. Hawking, *Black holes in the early Universe*, *Mon. Not. Roy. Astron. Soc.* **168** (1974) 399.
- [47] S. Wang, T. Terada and K. Kohri, *Prospective constraints on the primordial black hole abundance from the stochastic gravitational-wave backgrounds produced by coalescing events and curvature perturbations*, *Phys. Rev. D* **99** (2019) 103531 [1903.05924].
- [48] C.T. Byrnes and P.S. Cole, *Lecture notes on inflation and primordial black holes*, 12, 2021 [2112.05716].
- [49] M. Braglia, A. Linde, R. Kallosh and F. Finelli, *Hybrid α -attractors, primordial black holes and gravitational wave backgrounds*, 2211.14262.
- [50] Y.-P. Wu, E. Pinetti and J. Silk, *Cosmic Coincidences of Primordial-Black-Hole Dark Matter*, *Phys. Rev. Lett.* **128** (2022) 031102 [2109.09875].
- [51] M. Crawford and D.N. Schramm, *Spontaneous Generation of Density Perturbations in the*

- Early Universe*, *Nature* **298** (1982) 538.
- [52] S.W. Hawking, I.G. Moss and J.M. Stewart, *Bubble Collisions in the Very Early Universe*, *Phys. Rev. D* **26** (1982) 2681.
- [53] I.G. Moss, *Singularity formation from colliding bubbles*, *Phys. Rev. D* **50** (1994) 676.
- [54] H. Kodama, M. Sasaki and K. Sato, *Abundance of Primordial Holes Produced by Cosmological First Order Phase Transition*, *Prog. Theor. Phys.* **68** (1982) 1979.
- [55] M.J. Baker, M. Breitbach, J. Kopp and L. Mittnacht, *Primordial Black Holes from First-Order Cosmological Phase Transitions*, [2105.07481](#).
- [56] K. Kawana and K.-P. Xie, *Primordial black holes from a cosmic phase transition: The collapse of Fermi-balls*, *Phys. Lett. B* **824** (2022) 136791 [[2106.00111](#)].
- [57] P. Huang and K.-P. Xie, *Primordial black holes from an electroweak phase transition*, *Phys. Rev. D* **105** (2022) 115033 [[2201.07243](#)].
- [58] K. Hashino, S. Kanemura and T. Takahashi, *Primordial black holes as a probe of strongly first-order electroweak phase transition*, *Phys. Lett. B* **833** (2022) 137261 [[2111.13099](#)].
- [59] J. Liu, L. Bian, R.-G. Cai, Z.-K. Guo and S.-J. Wang, *Primordial black hole production during first-order phase transitions*, *Phys. Rev. D* **105** (2022) L021303 [[2106.05637](#)].
- [60] Y. Gouttenoire and T. Volansky, *Primordial Black Holes from Supercooled Phase Transitions*, [2305.04942](#).
- [61] M. Lewicki, P. Toczek and V. Vaskonen, *Primordial black holes from strong first-order phase transitions*, *JHEP* **09** (2023) 092 [[2305.04924](#)].
- [62] T.C. Gehrman, B. Shams Es Haghi, K. Sinha and T. Xu, *Recycled Dark Matter*, [2310.08526](#).
- [63] T. Kim, P. Lu, D. Marfatia and V. Takhistov, *Regurgitated Dark Matter*, [2309.05703](#).
- [64] D. Borah, S. Jyoti Das and I. Saha, *Dark matter from phase transition generated PBH evaporation with gravitational waves signatures*, *Phys. Rev. D* **110** (2024) 035014 [[2401.12282](#)].
- [65] S.W. Hawking, *Black Holes From Cosmic Strings*, *Phys. Lett. B* **231** (1989) 237.
- [66] H. Deng, J. Garriga and A. Vilenkin, *Primordial black hole and wormhole formation by domain walls*, *JCAP* **04** (2017) 050 [[1612.03753](#)].
- [67] D. Marfatia and P.-Y. Tseng, *Correlated signals of first-order phase transitions and primordial black hole evaporation*, *JHEP* **08** (2022) 001 [[2112.14588](#)].

- [68] P.-Y. Tseng and Y.-M. Yeh, *511 keV line and primordial black holes from first-order phase transitions*, *JCAP* **08** (2023) 035 [[2209.01552](#)].
- [69] P. Lu, K. Kawana and A. Kusenko, *Late-forming primordial black holes: Beyond the CMB era*, *Phys. Rev. D* **107** (2023) 103037 [[2210.16462](#)].
- [70] D. Marfatia and P.-Y. Tseng, *Boosted dark matter from primordial black holes produced in a first-order phase transition*, *JHEP* **04** (2023) 006 [[2212.13035](#)].
- [71] K.-P. Xie, *Pinning down the primordial black hole formation mechanism with gamma-rays and gravitational waves*, *JCAP* **06** (2023) 008 [[2301.02352](#)].
- [72] S.M. Davidson and H.E. Logan, *Dirac neutrinos from a second Higgs doublet*, *Phys. Rev. D* **80** (2009) 095008 [[0906.3335](#)].
- [73] S. Kanemura, T. Matsui and H. Sugiyama, *Loop Suppression of Dirac Neutrino Mass in the Neutrinophilic Two Higgs Doublet Model*, *Phys. Lett. B* **727** (2013) 151 [[1305.4521](#)].
- [74] S.R. Coleman and E.J. Weinberg, *Radiative Corrections as the Origin of Spontaneous Symmetry Breaking*, *Phys. Rev. D* **7** (1973) 1888.
- [75] L. Dolan and R. Jackiw, *Symmetry Behavior at Finite Temperature*, *Phys. Rev. D* **9** (1974) 3320.
- [76] M. Quiros, *Finite temperature field theory and phase transitions*, in *ICTP Summer School in High-Energy Physics and Cosmology*, pp. 187–259, 1, 1999 [[hep-ph/9901312](#)].
- [77] P. Fendley, *The Effective Potential and the Coupling Constant at High Temperature*, *Phys. Lett. B* **196** (1987) 175.
- [78] R.R. Parwani, *Resummation in a hot scalar field theory*, *Phys. Rev. D* **45** (1992) 4695 [[hep-ph/9204216](#)].
- [79] P.B. Arnold and O. Espinosa, *The Effective potential and first order phase transitions: Beyond leading-order*, *Phys. Rev. D* **47** (1993) 3546 [[hep-ph/9212235](#)].
- [80] A.D. Linde, *Fate of the False Vacuum at Finite Temperature: Theory and Applications*, *Phys. Lett. B* **100** (1981) 37.
- [81] J. Ellis, M. Lewicki and J.M. No, *On the Maximal Strength of a First-Order Electroweak Phase Transition and its Gravitational Wave Signal*, *JCAP* **04** (2019) 003 [[1809.08242](#)].
- [82] J. Ellis, M. Lewicki and V. Vaskonen, *Updated predictions for gravitational waves produced in a strongly supercooled phase transition*, *JCAP* **11** (2020) 020 [[2007.15586](#)].
- [83] C. Caprini et al., *Detecting gravitational waves from cosmological phase transitions with*

- LISA: an update*, *JCAP* **03** (2020) 024 [[1910.13125](#)].
- [84] M. Kamionkowski, A. Kosowsky and M.S. Turner, *Gravitational radiation from first order phase transitions*, *Phys. Rev. D* **49** (1994) 2837 [[astro-ph/9310044](#)].
- [85] P.J. Steinhardt, *Relativistic Detonation Waves and Bubble Growth in False Vacuum Decay*, *Phys. Rev. D* **25** (1982) 2074.
- [86] J.R. Espinosa, T. Konstandin, J.M. No and G. Servant, *Energy Budget of Cosmological First-order Phase Transitions*, *JCAP* **06** (2010) 028 [[1004.4187](#)].
- [87] F.C. Adams, *General solutions for tunneling of scalar fields with quartic potentials*, *Phys. Rev. D* **48** (1993) 2800 [[hep-ph/9302321](#)].
- [88] M.J. Baker, J. Kopp and A.J. Long, *Filtered Dark Matter at a First Order Phase Transition*, *Phys. Rev. Lett.* **125** (2020) 151102 [[1912.02830](#)].
- [89] D. Chway, T.H. Jung and C.S. Shin, *Dark matter filtering-out effect during a first-order phase transition*, *Phys. Rev. D* **101** (2020) 095019 [[1912.04238](#)].
- [90] D. Marfatia and P.-Y. Tseng, *Gravitational wave signals of dark matter freeze-out*, *JHEP* **02** (2021) 022 [[2006.07313](#)].
- [91] W. Chao, X.-F. Li and L. Wang, *Filtered pseudo-scalar dark matter and gravitational waves from first order phase transition*, *JCAP* **06** (2021) 038 [[2012.15113](#)].
- [92] M. Ahmadvand, *Filtered asymmetric dark matter during the Peccei-Quinn phase transition*, *JHEP* **10** (2021) 109 [[2108.00958](#)].
- [93] M.J. Baker, M. Breitbach, J. Kopp, L. Mitnacht and Y. Soreq, *Filtered baryogenesis*, *JHEP* **08** (2022) 010 [[2112.08987](#)].
- [94] S. Jiang, F.P. Huang and C.S. Li, *Hydrodynamic effects on the filtered dark matter produced by a first-order phase transition*, *Phys. Rev. D* **108** (2023) 063508 [[2305.02218](#)].
- [95] P. Asadi, E.D. Kramer, E. Kuflik, G.W. Ridgway, T.R. Slatyer and J. Smirnov, *Thermal squeezeout of dark matter*, *Phys. Rev. D* **104** (2021) 095013 [[2103.09827](#)].
- [96] J. Arakawa, A. Rajaraman and T.M.P. Tait, *Annihilogenesis*, *JHEP* **08** (2022) 078 [[2109.13941](#)].
- [97] T.D. Lee and Y. Pang, *Fermion Soliton Stars and Black Holes*, *Phys. Rev. D* **35** (1987) 3678.
- [98] J.-P. Hong, S. Jung and K.-P. Xie, *Fermi-ball dark matter from a first-order phase transition*, *Phys. Rev. D* **102** (2020) 075028 [[2008.04430](#)].

- [99] L. Del Grosso, G. Franciolini, P. Pani and A. Urbano, *Fermion soliton stars*, *Phys. Rev. D* **108** (2023) 044024 [2301.08709].
- [100] B.J. Carr, K. Kohri, Y. Sendouda and J. Yokoyama, *New cosmological constraints on primordial black holes*, *Phys. Rev. D* **81** (2010) 104019 [0912.5297].
- [101] B.V. Lehmann, S. Profumo and J. Yant, *The Maximal-Density Mass Function for Primordial Black Hole Dark Matter*, *JCAP* **04** (2018) 007 [1801.00808].
- [102] H. Niikura et al., *Microlensing constraints on primordial black holes with Subaru/HSC Andromeda observations*, *Nature Astron.* **3** (2019) 524 [1701.02151].
- [103] K. Griest and M. Kamionkowski, *Unitarity Limits on the Mass and Radius of Dark Matter Particles*, *Phys. Rev. Lett.* **64** (1990) 615.
- [104] LISA collaboration, *Laser Interferometer Space Antenna*, *arXiv e-prints* (2017) arXiv:1702.00786 [1702.00786].
- [105] M.S. Turner and F. Wilczek, *Relic gravitational waves and extended inflation*, *Phys. Rev. Lett.* **65** (1990) 3080.
- [106] A. Kosowsky, M.S. Turner and R. Watkins, *Gravitational radiation from colliding vacuum bubbles*, *Phys. Rev. D* **45** (1992) 4514.
- [107] A. Kosowsky, M.S. Turner and R. Watkins, *Gravitational waves from first order cosmological phase transitions*, *Phys. Rev. Lett.* **69** (1992) 2026.
- [108] A. Kosowsky and M.S. Turner, *Gravitational radiation from colliding vacuum bubbles: envelope approximation to many bubble collisions*, *Phys. Rev. D* **47** (1993) 4372 [astro-ph/9211004].
- [109] M.S. Turner, E.J. Weinberg and L.M. Widrow, *Bubble nucleation in first order inflation and other cosmological phase transitions*, *Phys. Rev. D* **46** (1992) 2384.
- [110] M. Hindmarsh, S.J. Huber, K. Rummukainen and D.J. Weir, *Gravitational waves from the sound of a first order phase transition*, *Phys. Rev. Lett.* **112** (2014) 041301 [1304.2433].
- [111] J.T. Giblin and J.B. Mertens, *Gravitational radiation from first-order phase transitions in the presence of a fluid*, *Phys. Rev. D* **90** (2014) 023532 [1405.4005].
- [112] M. Hindmarsh, S.J. Huber, K. Rummukainen and D.J. Weir, *Numerical simulations of acoustically generated gravitational waves at a first order phase transition*, *Phys. Rev. D* **92** (2015) 123009 [1504.03291].
- [113] M. Hindmarsh, S.J. Huber, K. Rummukainen and D.J. Weir, *Shape of the acoustic*

- gravitational wave power spectrum from a first order phase transition*, *Phys. Rev. D* **96** (2017) 103520 [[1704.05871](#)].
- [114] A. Kosowsky, A. Mack and T. Kahniashvili, *Gravitational radiation from cosmological turbulence*, *Phys. Rev. D* **66** (2002) 024030 [[astro-ph/0111483](#)].
- [115] C. Caprini and R. Durrer, *Gravitational waves from stochastic relativistic sources: Primordial turbulence and magnetic fields*, *Phys. Rev. D* **74** (2006) 063521 [[astro-ph/0603476](#)].
- [116] G. Gogoberidze, T. Kahniashvili and A. Kosowsky, *The Spectrum of Gravitational Radiation from Primordial Turbulence*, *Phys. Rev. D* **76** (2007) 083002 [[0705.1733](#)].
- [117] C. Caprini, R. Durrer and G. Servant, *The stochastic gravitational wave background from turbulence and magnetic fields generated by a first-order phase transition*, *JCAP* **12** (2009) 024 [[0909.0622](#)].
- [118] P. Niksa, M. Schlexer and G. Sigl, *Gravitational Waves produced by Compressible MHD Turbulence from Cosmological Phase Transitions*, *Class. Quant. Grav.* **35** (2018) 144001 [[1803.02271](#)].
- [119] K. Yagi and N. Seto, *Detector configuration of DECIGO/BBO and identification of cosmological neutron-star binaries*, *Phys. Rev. D* **83** (2011) 044011 [[1101.3940](#)].
- [120] A. Sesana et al., *Unveiling the gravitational universe at μ -Hz frequencies*, *Exper. Astron.* **51** (2021) 1333 [[1908.11391](#)].
- [121] D.E. Kaplan, M.A. Luty and K.M. Zurek, *Asymmetric Dark Matter*, *Phys. Rev. D* **79** (2009) 115016 [[0901.4117](#)].
- [122] A. Falkowski, J.T. Ruderman and T. Volansky, *Asymmetric Dark Matter from Leptogenesis*, *JHEP* **05** (2011) 106 [[1101.4936](#)].
- [123] A. Biswas, S. Choubey, L. Covi and S. Khan, *Common origin of baryon asymmetry, dark matter and neutrino mass*, *JHEP* **05** (2019) 193 [[1812.06122](#)].
- [124] N. Narendra, S. Patra, N. Sahu and S. Shil, *Baryogenesis via Leptogenesis from Asymmetric Dark Matter and radiatively generated Neutrino mass*, *Phys. Rev. D* **98** (2018) 095016 [[1805.04860](#)].
- [125] N. Nagata, K.A. Olive and J. Zheng, *Asymmetric Dark Matter Models in $SO(10)$* , *JCAP* **02** (2017) 016 [[1611.04693](#)].
- [126] C. Arina and N. Sahu, *Asymmetric Inelastic Inert Doublet Dark Matter from Triplet Scalar*

- Leptogenesis*, *Nucl. Phys. B* **854** (2012) 666 [[1108.3967](#)].
- [127] C. Arina, J.-O. Gong and N. Sahu, *Unifying darko-lepto-genesis with scalar triplet inflation*, *Nucl. Phys. B* **865** (2012) 430 [[1206.0009](#)].
- [128] C. Arina, R.N. Mohapatra and N. Sahu, *Co-genesis of Matter and Dark Matter with Vector-like Fourth Generation Leptons*, *Phys. Lett. B* **720** (2013) 130 [[1211.0435](#)].
- [129] N. Narendra, N. Sahu and S. Shil, *Dark matter to baryon ratio from scalar triplets decay in type-II seesaw*, *Eur. Phys. J. C* **81** (2021) 1098 [[1910.12762](#)].
- [130] S. Mahapatra, P.K. Paul, N. Sahu and P. Shukla, *Asymmetric long-lived dark matter and leptogenesis from the type-III seesaw framework*, *Phys. Rev. D* **111** (2025) 015043 [[2305.11138](#)].
- [131] A. Lloyd-Stubbs and J. McDonald, *A Minimal Approach to Baryogenesis via Affleck-Dine and Inflaton Mass Terms*, *Phys. Rev. D* **103** (2021) 123514 [[2008.04339](#)].
- [132] R.N. Mohapatra and N. Okada, *Affleck-Dine baryogenesis with observable neutron-antineutron oscillation*, *Phys. Rev. D* **104** (2021) 055030 [[2107.01514](#)].
- [133] J.B. Dent, B. Dutta and T. Xu, *Multi-messenger probes of asteroid mass primordial black holes: Superradiance spectroscopy, Hawking radiation, and microlensing*, *Phys. Lett. B* **861** (2025) 139254 [[2404.02956](#)].